IEEJ Journal of Industry Applications
Vol.15 No.2 pp.161–172 DOI: 10.1541/ieejjia.20250046

Paper

On Convergence, Tracking-performance and Task-flexibility of Joint Parametrized/Signal-based Iterative Learning Control

Kentaro Tsurumoto[*a)] Student Member, Wataru Ohnishi[*] Senior Member
Takafumi Koseki[*] Fellow, Johan Kon[**] Non-member
Maurice Poot[**] Non-member, Tom Oomen[**,***] Non-member

(Manuscript received April 17, 2025, revised July 29, 2025)
J-STAGE Advance published date : Dec. 26, 2025

Many industrial motion systems require performing a variety of tasks with high precision and safety. Iterative learning control (ILC) is a method with convergent update laws, generally classified into: 1) parametrized learning approach for achieving task-flexibility against varying tasks; or 2) signal-based learning approach which can achieve perfect tracking-performance for repeating tasks. The aim of this study is to join the distinct ILC frameworks, achieving all desirable properties in a single framework. Specifications on convergence, tracking-performance and task-flexibility of the developed joint parametrized/signal-based ILC are theoretically derived, confirmed with experimental results on a two-mass system.

Keywords: feedforward control, iterative learning control, basis functions, frequency-domain design

1. Introduction

Feedforward (FF) control in industrial motion systems are crucial for achieving high-speed and high-tracking performance. Especially, for high-precision mechatronics systems, e.g., semiconductor lithography[(1)], machine tools[(2)], and industrial robots[(3)], exceptionally accurate and reliable FF control based on an accurate system model is essential[(4)(5)].

Iterative learning control (ILC)[(6)–(8)] is a data-based control method applied to enhance the tracking-performance of systems with batch-wise repetitive operations. In ILC, without requiring a specific accurate system model, an accurate FF input is learned in a convergent manner utilizing data from past experiments. Compared to adaptive control schemes[(9)] and feedback controller optimization methods[(10)], ILC offers the advantages of generally more relaxed convergence conditions and overcome performance limitations imposed by Bode's integral theorem. However, its applicability is fundamentally restricted to systems only performing batch-wise repetitive operations.

ILC can be classified into two categories; parametrized or signal-based FF input learning. The concept of a parametrized and signal-based FF input is illustrated in Fig. 1. Typically in parametrized ILC frameworks such as basis function ILC (B-ILC)[(11)(12)], the parameters associated with the physical properties of the system (e.g., velocity, acceleration, snap) are learned and combined linearly to construct a FF input. This leads to parametrized ILC frameworks having high task-flexibility against trial-varying references. However, typically due to the learned parameters only being sufficient (and not perfect) to represent the entire dynamics of the system, perfect-tracking cannot be achieved. In contrast, in signal-based ILC frameworks such as frequency-domain ILC (F-ILC)[(13)–(15)], the FF input is constructed directly applying the filtered error result obtained from the previous test. This leads to a FF input that further enhances tracking-performance, due to the increase in expressivity in dynamics. However, as this can be interpreted as the exploitation of

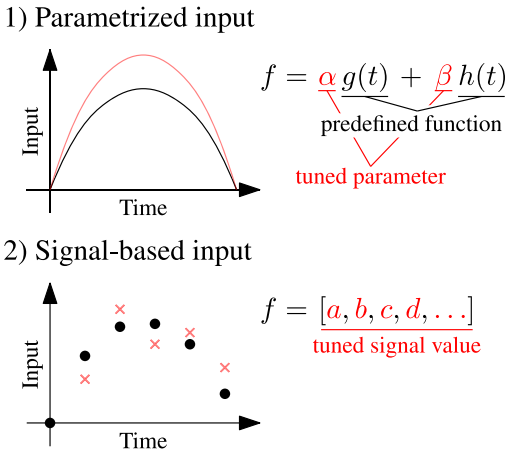

Fig. 1. Concept of learning for parametrized and signal-based FF input

a) Correspondence to: Kentaro Tsurumoto. E-mail: k.tsurumoto@ctl.t.u-tokyo.ac.jp
* Department of Electrical Engineering and Information Systems, The University of Tokyo
7-3-1, Hongo, Bunkyo-ku, Tokyo 113-8656, Japan
** Department of Mechanical Engineering, Eindhoven University of Technology
Eindhoven, Netherlands
*** Delft Center for Systems and Control, Delft University of Technology
Delft, Netherlands

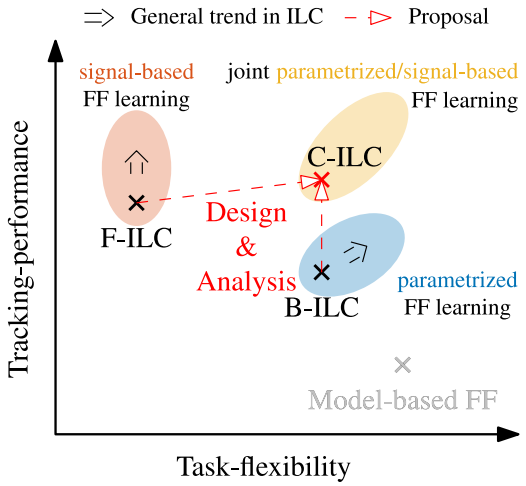

Fig. 2. Trade-off between tracking-performance and task-flexibility in ILC[30][33]. In this study, ILC combining parametrized ILC (originating from B-ILC) with signal-based ILC (originating from F-ILC) is considered

overfitting to a specific trial-invariant reference, signal-based ILC frameworks lack task-flexibility against trial-varying references.

Recent developments in ILC have included: 1) establishment of design guidelines to assure robust monotonic convergence[16]; 2) suppression of trial-variant disturbances[17]–[19]; 3) incorporation of input and output constraints[20][21]; 4) improvement of intersample performance[22]–[24]; 5) advances in model-free learning[25]–[27]; and 6) utilization of machine learning frameworks for enhanced task flexibility[28][29]. These efforts have individually extended the capabilities of parametrized and signal-based ILC frameworks. In contrast, not much focus has been given to join parametrized and signal-based ILC together to achieve the strengths of both frameworks (Fig. 2).

One of the major challenges in joining distinct ILC frameworks is how to avoid interference from parallel learning. For instance, naively combining distinct ILC frameworks typically lead to divergent learning results, regardless of each ILC design being convergent when used alone. An attempt to avoiding this divergent learning behavior is presented in study (30)–(32), proposing an combined ILC (C-ILC) framework complementarily combining parametrized ILC with signal-based ILC. However, specific analysis on: 1) why the designed complementarily combination scheme is motivated for decoupling the interaction between parametrized and signal-based ILC; and 2) derivation on the condition when the developed framework is beneficial (compared to only using parametrized ILC or signal-based ILC); has been lacking.

The aim of this study is to: 1) provide a detailed guideline on the design of complementarily joint parametrized/signal-based ILC framework; and 2) theoretically specify when the joint parametrized/signal-based ILC yields the most desirable results, i.e., convergent learning with high task-flexibility as that of parametrized ILC and high tracking-performance exceeding that of signal-based ILC. This study extends the results reported in study (30), providing theoretical specification on convergence, tracking-performance and task-flexibility, verified with experimental validation. In terms of novelty in this study, the unanswered questions in study (30) are considered by: 1) investigating the case of naively combining B-ILC and F-ILC update laws, leading to undesirable divergent learning; and 2) investigating the influence of modeling error in the learning of joint parametrized/signal-based ILC.

The key contributions of this study on the design and analysis of joint parametrized/signal-based ILC are summarized as follows.

C1 Presenting a framework for joint parametrized/signal-based ILC and proving its convergence, tracking-performance and task-flexibility. (Section 4)

C2 Experimentally verifying the potential of joint parametrized/signal-based ILC being maximized under insufficient modeling scenarios. (Section 5)

C3 Formulating the divergent learning behavior caused by naively combining the update laws of parametrized and signal-based ILC. (Section 2.5)

Note that in this study, as a basic example of joint parametrized/signal-based ILC, the specific combination of B-ILC and F-ILC (introduced as combined ILC (C-ILC) in study (30)) is considered.

1.1 Notation Let $H(z) \in \mathcal{R}^{1\times1}$ denote a discrete-time single-input single-output (SISO) transfer function. The frequency response function of $H(z)$ is obtained by substituting $z = e^{i\omega}\ \forall\omega \in [0, 2\pi)$, and is denoted by $H(e^{i\omega})$. Throughout this paper (z) is omitted when clear from the context, and $\hat{H}$ is a model of H. The input and output of H are u and y, and the signal length is assumed as $N \in \mathbb{N}$.

Let $h(t)$ be the impulse response of H. The finite-time convolution matrix $H_{N\times N} \in \mathbb{R}^{N\times N}$ corresponding to H is

$$\underbrace{\begin{bmatrix} y(0) \\ y(1) \\ \vdots \\ y(N-1) \end{bmatrix}}_{\underline{y}} = \underbrace{\begin{bmatrix} h(0) & h(-1) & \cdots & h(1-N) \\ h(1) & h(0) & \cdots & h(2-N) \\ \vdots & \vdots & \ddots & \vdots \\ h(N-1) & h(N-2) & \cdots & h(0) \end{bmatrix}}_{H_{N\times N}} \underbrace{\begin{bmatrix} u(0) \\ u(1) \\ \vdots \\ u(N-1) \end{bmatrix}}_{\underline{u}},$$

where $\underline{u} \in \mathbb{R}^{N\times1}$ and $\underline{y} \in \mathbb{R}^{N\times1}$ denote N sample lifted vectors of u and y, assuming zero initial and final conditions. Note that the resulting outputs of time-domain representation $\underline{y} = H_{N\times N}\,\underline{u}$ and frequency-domain representation $y = Hu$ are equivalent on any finite time interval when H is stable and causal.

Additionally, $\bar{\sigma}(A)$ denotes the maximum singular value of matrix A, a weighted two norm for vector x is given by $\|x\|_W^2 = x^\top W x$, a positive definite matrix A is denoted as $A > 0$, and $I_{N\times N}$ is an $N \times N$ identity matrix.

2. Problem Formulation

In this section the considered problem is defined by describing the system, and introducing F-ILC and B-ILC.

2.1 Two-mass Motion System High-precision positioning stages, often used in industrial fields such as semiconductor manufacturing, can typically be modeled as a two-mass motion system illustrated in Fig. 3[34][35]. While flexible modes of the system are often a limiting factor

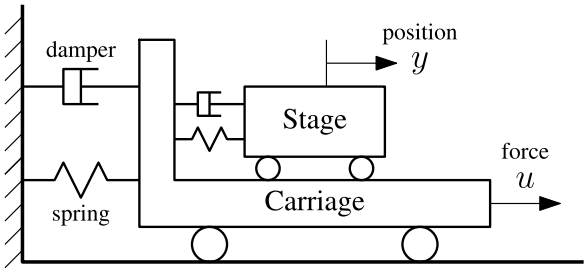

Fig. 3. Model of high-precision motion system

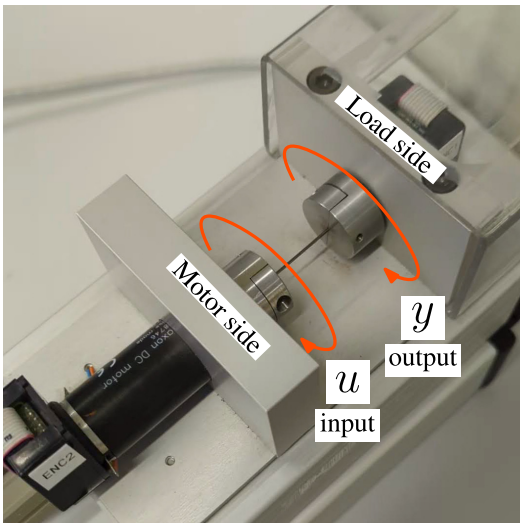

Fig. 4. Experimental setup of two-mass motion system

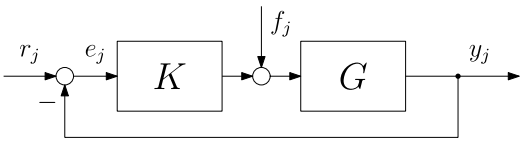

Fig. 5. Block diagram of considered closed-loop system. j denotes the iteration number of the motion task

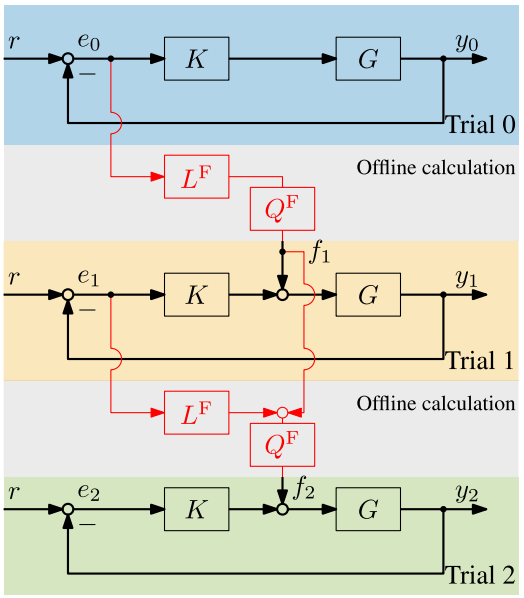

Fig. 6. Update scheme of frequency-domain ILC (F-ILC). The flow of the frequency-domain learning is denoted by (→)

for performance, typical motion systems are designed such that flexible modes are far beyond the target bandwidth. However, increasing performance requirements necessitate larger bandwidth for next-generation mechatronic systems, which requires the consideration of flexible modes[36].

In this study, controlling a two-mass motion system presented in Fig. 4 is considered. The system consists of a current-controlled DC-motor driving a motor-side mass connected to a load-side mass via a flexible shaft. With the dynamics associated with the flexible connection of the two masses, the flexible mode of the high-precision positioning stages is simulated as shown later in the resonance in Fig. 9. In addition, due to nonlinear dynamics associated with friction and imbalance of the mass, frequency characteristics vary by operating point. Nonlinearity is a common difficulty in high-precision applications[37], adding significance on the experimental validation using this two-mass motion system.

2.2 System Description The control setup is shown in Fig. 5. Here system G and FB controller K are discrete-time SISO transfer functions. Subscript j denotes the iteration number of motion task, with r_j denoting the reference, f_j the feedforward input, y_j the measured output, and e_j the measured error given by

$$e_j = Sr_j - Jf_j, \cdots\cdots (1)$$

with sensitivity $S = (1 + GK)^{-1}$ and process sensitivity $J = SG$. To facilitate the presentation, for Sections 2, 3 and 4, $r = r_{j+1} = r_j$ is assumed.

2.3 Frequency-domain ILC (F-ILC) In this subsection, F-ILC[14][31] is introduced as an example of signal-based ILC.

The aim of F-ILC is to determine the feedforward input f_{j+1}, achieving perfect-tracking performance for trial-invariant reference, i.e., $r = r_{j+1} = r_j$. In F-ILC, this is achieved by designing f_{j+1} based on

$$f_{j+1} = Q^F(f_j + L^F e_j), \cdots\cdots (2)$$

with learning filter L^F and robustness filter Q^F designed by the user. Figure 6 shows the F-ILC input (f_j) update procedure for three iterations.

From (1) and (2), the propagation of error and FF input are expressed as

$$e_{j+1} = Q^F(1 - L^F J)e_j + (1 - Q^F)Sr, \cdots\cdots (3a)$$
$$f_{j+1} = Q^F(1 - L^F J)f_j + Q^F L^F Sr. \cdots\cdots (3b)$$

From (3), it is guaranteed that $\|e\|_2$ and $\|f\|_2$ converge monotonically within the entire frequency range ω when

$$|Q^F(e^{i\omega})(1 - L^F(e^{i\omega})J(e^{i\omega}))| < 1, \quad \forall\omega \in [0, \pi], \cdots (4)$$

is satisfied[14].

Remark 1 An advantage of frequency-domain design is that nonparametric frequency response data of J can be used for convergence analysis. By this analysis tool, the convergence of learning can be investigated before executing experiments.

When monotonic convergence condition (4) is satisfied, using (3), asymptotic error $\lim_{j\to\infty} e_j = e_\infty$ is derived as

$$e_\infty = \frac{(1 - Q^F)S}{1 - Q^F(1 - L^F J)} r, \cdots\cdots (5)$$

Remark 2 When (4) is satisfied with $Q^{\mathrm{F}} = 1$, perfect tracking $e_\infty = 0$ is achieved. For $Q^{\mathrm{F}} = 1$ to be applicable, $|1 - L^{\mathrm{F}}J| < 1$ is required. This motivates the design of $L^{\mathrm{F}} = \hat{J}^{-1} = \hat{G}^{-1}(1+\hat{G}K)$, with Q^{F} being a unity-magnitude lowpass filter with the highest bandwidth possible, not violating (4).

Remark 3 In the presence of significant trial-varying noise, setting $L^{\mathrm{F}} = \alpha\hat{J}^{-1}$ with a small learning gain $0 < \alpha \leq 1$ suppresses noise amplification. However, this typically slows convergence, requiring more experiment iterations.

2.4 Basis Function ILC (B-ILC) In this subsection, B-ILC[12][33] is introduced as an example of parametrized ILC.

The aim of B-ILC is to determine the feedforward input f_{j+1}, achieving high tracking performance even for tasks with trial-variant references, i.e., $r_{j+1} \neq r_j$. While signal-based ILC methods such as F-ILC can achieve perfect tracking for trial-invariant references, tracking performance can severely deteriorate for operations with nonrepetitive references[33]. Parametrized ILC frameworks such as B-ILC overcomes this problem by learning the parameters θ_{j+1} for the FF controller $F(\theta_{j+1})$, designed as

$$f_{j+1} = F(\theta_{j+1})r_{j+1}. \cdots\cdots (6)$$

Fig. 7 shows the B-ILC FF parameter (θ_j) update procedure for three iterations.

FF controller $F(\theta)$ is defined in Definition 1 by the user-defined basis functions $\Psi(z) \in \mathcal{R}^{n\times 1}$, where n denotes the number of basis.

Definition 1 (Parameterized FF controller) Given θ, the parameterized FF controller is constructed by

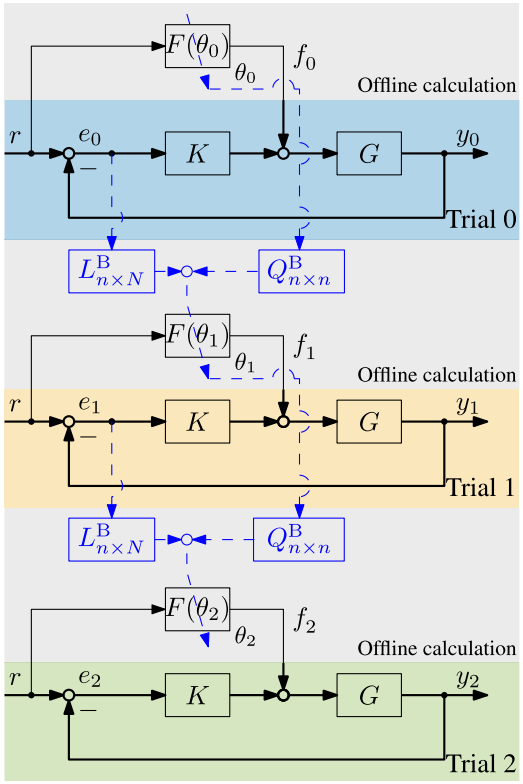

Fig. 7. Update scheme of basis function ILC (B-ILC). The flow of the time-domain learning is denoted by (-►)

$$F(\theta) = \sum_{i=0}^{n-1} \Psi[i]\theta[i]. \cdots\cdots (7)$$

Using (7), the time-domain representation of (6) is

$$\underline{f}_{j+1} = \Psi^{(r)}_{N\times n}\theta_{j+1}, \cdots\cdots (8)$$

where $\Psi^{(r)}_{N\times n} = [\underline{\Psi[0]r}, \underline{\Psi[1]r}, \cdots, \underline{\Psi[n-1]r}]$.

Remark 4 Definition 1 is a representation using polynomial basis functions, related to finite impulse response filter design. For enhanced system representation, rational basis functions[12][30][33] can be used.

FF parameters θ_{j+1} are determined by minimizing criterion $V(\theta_{j+1})$ defined in Definition 2.

Definition 2 (Criterion for B-ILC[12]) The performance criterion for B-ILC is given by

$$V(\theta_{j+1}) = \|\underline{\hat{e}}_{j+1}\|^2_{We} + \|\underline{f}_{j+1}\|^2_{Wf} + \|\underline{f}_{j+1} - \underline{f}_j\|^2_{W\Delta f}, \cdots\cdots (9)$$

where $W_e \succ 0$, $W_f \succeq 0$, and $W_{\Delta f} \succeq 0$ are user-defined weighting matrices and $\underline{\hat{e}}_{j+1} = \underline{e}_j + \hat{J}_{N\times N}(\underline{f}_j - \underline{f}_{j+1})$.

Remark 5 Typically, learning of B-ILC is sufficiently robust, only requiring the term $\|\underline{\hat{e}}_{j+1}\|^2_{We}$. Additional terms $\|\underline{f}_{j+1}\|^2_{Wf}$ and $\|\underline{f}_{j+1} - \underline{f}_j\|^2_{W\Delta f}$ can be utilized to enforce robustness in learning, later formulated in (13).

The corresponding FF parameter update is given by

$$\theta_{j+1} = \arg\min_{\theta_{j+1}} V(\theta_{j+1}), \cdots\cdots (10)$$

leading to the following optimal parameter update for B-ILC.

Lemma 1 (Optimal parameter update for B-ILC[12])
Optimal parameter update for B-ILC is formulated as

$$\theta_{j+1} = Q^{\mathrm{B}}_{n\times n}\theta_j + L^{\mathrm{B}}_{n\times N}\underline{e}_j, \cdots\cdots (11)$$

where

$$L^{\mathrm{B}}_{n\times N} = R^{-1}_{n\times n}\Psi^{(r)\top}_{N\times n}\hat{J}^{\top}_{N\times N}W_e, \cdots\cdots (12a)$$

$$Q^{\mathrm{B}}_{n\times n} = R^{-1}_{n\times n}\Psi^{(r)\top}_{N\times n}(\hat{J}^{\top}_{N\times N}W_e\hat{J}_{N\times N} + W_{\Delta f})\Psi^{(r)}_{N\times n}, \cdots\cdots (12b)$$

$$R_{n\times n} = \Psi^{(r)\top}_{N\times n}(\hat{J}^{\top}_{N\times N}W_e\hat{J}_{N\times N} + W_f + W_{\Delta f})\Psi^{(r)}_{N\times n},$$

Proof. The proof follows from standard norm-optimal ILC[38][39] with substitution of (8), satisfying the optimality condition $\partial V(\theta_{j+1})/\partial\theta_{j+1} = 0$. □

Remark 6 Note that $L^{\mathrm{B}}_{n\times N}$ and $Q^{\mathrm{B}}_{n\times n}$ are not necessarily convolution matrices for any LTI filter.

Remark 7 Although B-ILC enhances the extrapolation properties of ILC, system G often include dynamics unmodeled by (7), e.g., system zeros and nonlinearity. From (1), this leads to $e_\infty \neq 0$, typically larger than the error of F-ILC derived in (5), against trial-invariant references.

From (1), (8), and (11) monotonic convergence of $\|\theta\|_2$ is satisfied[40] when

$$\bar{\sigma}(Q^{\mathrm{B}}_{n\times n} - L^{\mathrm{B}}_{n\times N}J_{N\times N}\Psi^{(r)}_{N\times n}) < 1, \cdots\cdots (13)$$

and the asymptotic FF parameter $\lim_{j\to\infty}\theta_j = \theta_\infty$ is derived as

$$\theta_\infty = (I_{n\times n} - Q^{\mathrm{B}}_{n\times n} + L^{\mathrm{B}}_{n\times N}J_{N\times N}\Psi^{(r)}_{N\times n})^{-1}L^{\mathrm{B}}_{n\times N}S_{N\times N}\underline{r}. \cdots\cdots (14)$$

2.5 Naively Combining F-ILC with B-ILC Assume

constructing

$$\underline{f}_{j+1} = \underline{f}^{\mathrm{F}}_{j+1} + \underline{f}^{\mathrm{B}}_{j+1} = \underline{f}^{\mathrm{F}}_{j+1} + \Psi^{(r)}_{N\times n}\theta_{j+1}, \cdots\cdots\cdots (15)$$

using updates

$$\underline{f}^{\mathrm{F}}_{j+1} = \underline{f}^{\mathrm{F}}_{j} + L^{\mathrm{F}}_{N\times N}\underline{e}_j, \cdots\cdots\cdots (16)$$

$$\Psi^{(r)}_{N\times n}\theta_{j+1} = \Psi^{(r)}_{N\times n}\theta_j + \Psi^{(r)}_{N\times n}L^{\mathrm{B}}_{n\times N}\underline{e}_j, \cdots\cdots\cdots (17)$$

derived from (2) and (11), respectively. To facilitate the presentation, it is assumed that (4) and (13) are satisfied with $Q^{\mathrm{F}} = 1$ and $Q^{\mathrm{B}}_{n\times n} = I_{n\times n}$.

From (1), (15), (16) and (17), the propagation of error for naively combining F-ILC and B-ILC is derived as

$$\underline{e}_{j+1} = (I_{N\times N} - J_{N\times N}L^{\mathrm{F}}_{N\times N} - J_{N\times N}\Psi^{(r)}_{N\times n}L^{\mathrm{B}}_{n\times N})\underline{e}_j, \cdots (18)$$

with the monotonic convergence condition of $\|e\|_2$ being

$$\bar{\sigma}(I_{N\times N} - J_{N\times N}L^{\mathrm{F}}_{N\times N} - J_{N\times N}\Psi^{(r)}_{N\times n}L^{\mathrm{B}}_{n\times N}) < 1. \cdots (19)$$

However, from the triangular inequality of matrix norms

$$\bar{\sigma}(I_{N\times N} - J_{N\times N}L^{\mathrm{F}}_{N\times N} - J_{N\times N}\Psi^{(r)}_{N\times n}L^{\mathrm{B}}_{n\times N})$$
$$\leq \bar{\sigma}(I_{N\times N} - J_{N\times N}L^{\mathrm{F}}_{N\times N}) + \bar{\sigma}(J_{N\times N}\Psi^{(r)}_{N\times n}L^{\mathrm{B}}_{n\times N}), \cdots (20)$$

and $\bar{\sigma}(J_{N\times N}\Psi^{(r)}_{N\times n}L^{\mathrm{B}}_{n\times N}) \approx 1$, it is not guaranteed that (19) is satisfied with

$$\bar{\sigma}(I_{N\times N} - J_{N\times N}L^{\mathrm{F}}_{N\times N}) < 1, \cdots\cdots\cdots (21)$$

which is equivalent to the monotonic convergence condition (4) under $Q^{\mathrm{F}} = 1$, when L^{F} is stable and causal[14].

Remark 8 In fact, (19) is violated for typical setups, causing divergent learning behavior demonstrated in Appendix 1.

2.6 Problem Description The problem addressed in this study is to develop a joint ILC framework combining the signal-based ILC and parametrized ILC design as (15), in a complementary manner. For the joint parametrized/signal-based ILC framework: 1) perfect tracking capability against repetitive tasks ($r_{j+1} = r_j$); alongside 2) high task flexibility for nonrepetitive tasks ($r_{j+1} \neq r_j$); are desired. However, naively combining signal-based ILC with parametrized ILC leads to divergent learning. The objective of joint parametrized/signal-based ILC is to modify the update law for signal-based FF input f^{F} in (16) and signal-based FF input f^{B} in (17) to achieve complementary learning. The aim of this study is to analyze the properties on convergence, tracking-performance and task-flexibility of joint parametrized/signal-based ILC.

3. Joint Parameterized/Signal-based ILC

In this section, C-ILC, the joint parametrized/signal-based ILC framework introduced in study (30) is presented. The C-ILC framework complementarily combines the update of parametrized FF input f^{B}_{j+1} (originating from B-ILC) and signal-based FF input f^{F}_{j+1} (originating from F-ILC). The entire scheme is presented in Procedure 1 and illustrated in Fig. 8.

3.1 Learning of Parametrized FF input f^{B}_{j+1} The

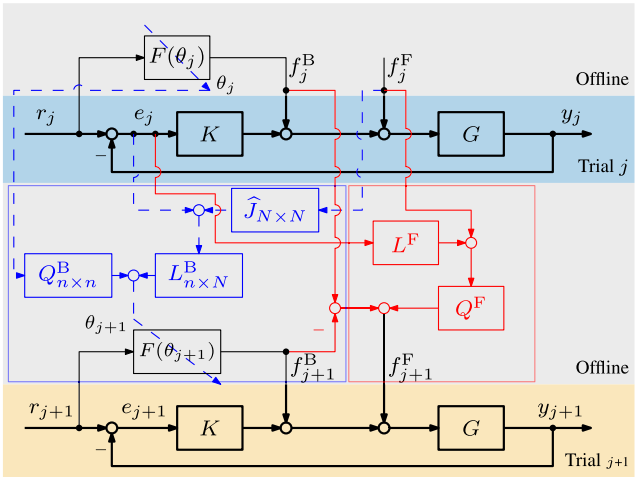

Fig. 8. Update scheme of combined ILC (C-ILC). The flow of the time-domain update for f^{B}_{j+1} (-►) and frequency-domain update for f^{F}_{j+1} (→) are illustrated

aim of learning $f^{\mathrm{B}}_{j+1} = F(\theta_{j+1})r$ in C-ILC is to ensure as high task-flexibility as that of B-ILC. In B-ILC, task-flexibility is achieved by minimizing criterion (9), with its main contribution being regularization of error

$$e_{j+1} = S(1 - GF(\theta_{j+1}))r, \cdots\cdots\cdots (22)$$

leading to $F(\theta_{j+1}) \approx G^{-1}$. However, when FF learning is combined as $f_{j+1} = f^{\mathrm{F}}_{j+1} + f^{\mathrm{B}}_{j+1}$ in (15), the error results in

$$e_{j+1} = S(1 - GF(\theta_{j+1}))r - Jf^{\mathrm{F}}_{j+1}, \cdots\cdots\cdots (23)$$

not necessarily leading to $F(\theta_{j+1}) \approx G^{-1}$ due to the existence of f^{F}_{j+1}. Therefore, for the parametrized FF learning of C-ILC, minimizing the criterion modified as Definition 3 is proposed.

Definition 3 (Criterion for f^{B}_{j+1}) The performance criterion for C-ILC is given by

$$V(\theta_{j+1}) = \|\underline{\hat{e}}^{\theta}_{j+1}\|^2_{We} + \|\underline{f}^{\mathrm{B}}_{j+1}\|^2_{Wf} + \|\underline{f}^{\mathrm{B}}_{j+1} - \underline{f}^{\mathrm{B}}_{j}\|^2_{W\Delta f}, \cdots\cdots\cdots (24)$$

where the first term of (9) is replaced with

$$\underline{\hat{e}}^{\theta}_{j+1} = \underline{\hat{e}}_{j+1} + \hat{J}\underline{f}^{\mathrm{F}}_{j+1}$$
$$= \underline{e}_j + \hat{J}(\underline{f}^{\mathrm{B}}_{j} - \underline{f}^{\mathrm{B}}_{j+1}), \cdots\cdots\cdots (25)$$

the estimated virtual error solely induced by f^{B}_{j+1}.

Introducing the regularization of virtual error derived as

$$e^{\theta}_{j+1} = S(1 - GF(\theta_{j+1}))r, \cdots\cdots\cdots (26)$$

this results to $F(\theta_{j+1}) \approx G^{-1}$ identical to that of B-ILC. This desirable property will later be discussed in Section 4, further demonstrated in Figs. 12 and 15. As a consequence of modifying the criterion, this leads to the following optimal parameter update for C-ILC.

Definition 4 (Optimal parameter update for f^{B}_{j+1}) Optimal parameter update for C-ILC is formulated as

$$\theta_{j+1} = Q^{\mathrm{B}}_{n\times n}\theta_j + L^{\mathrm{B}}_{n\times N}(\underline{e}_j + \hat{J}_{N\times N}\underline{f}^{\mathrm{F}}_{j}), \cdots\cdots\cdots (27)$$

where $Q^{\mathrm{B}}_{n\times n}$ and $L^{\mathrm{B}}_{n\times N}$ are same as in (12). For further derivation, see Appendix 2.

3.2 Learning of Signal-based FF Input f^{F}_{j+1} The

Procedure 1 (Update of C-ILC)

Define

- *Convolution matrix* $\hat{J}_{N\times N}$ *of process sensitivity model* $\hat{J}$
- *Basis function* $\Psi^{(r)}_{N\times n}$
- *Learning filter* L^{F} *and Robustness filter* Q^{F} *for signal-based FF learning*
- *Initial parametrized FF input* f^{B}_0 *based on initial FF parameter* θ_0*, and initial signal-based FF input* f^{F}_0

and start with $j = 0$.

(1) Perform the j^{th} *experiment and measure* e_j.

(2) Determine θ_{j+1} *based on (27).*

(3) Construct $f^{\mathrm{B}}_{j+1} = F(\theta_{j+1})r$.

(4) Construct f^{F}_{j+1} *based on (28).*

(4.1) Reset $f^{\mathrm{F}}_{j+1} = 0$ *when* $r_{j+1} \neq r_j$.
(This assures C-ILC to at least achieve identical task-flexibility as B-ILC.)

(5) Increment $j \to j+1$ *and return to Step (1).*

aim of learning f^{F}_{j+1} in C-ILC is to learn the residual dynamics uncaptured by f^{B}_{j+1} and achieve perfect tracking control against trial-invariant reference, i.e., $r = r_{j+1} = r_j$. Therefore, for the signal-based FF input of C-ILC, the FF update law defined as Definition 5 is proposed.

Definition 5 (Update of f^{F}_{j+1}) Update of f^{F}_{j+1} is given by

$$f^{\mathrm{F}}_{j+1} = Q^{\mathrm{F}}(f^{\mathrm{F}}_j + L^{\mathrm{F}}e_j) + f^{\mathrm{B}}_j - f^{\mathrm{B}}_{j+1}. \cdots\cdots\cdots\cdots \quad (28)$$

By adding the term $f^{\mathrm{B}}_j - f^{\mathrm{B}}_{j+1}$ to the standard update (2), f^{F}_{j+1} takes into account the dynamics already learned by f^{B}_{j+1}, leading to monotonic convergence of error $\|e\|_2$. This desirable property will be further discussed in Section 4.

Remark 9 Note that update (28) involves the term f^{B}_{j+1}, i.e., the basis function FF input for next iteration. However, this issue is resolved by calculating f^{B}_{j+1} beforehand, as in Procedure 1. As (27), calculation of f^{B}_{j+1} does not require f^{F}_{j+1}.

Remark 10 This developed framework can typically be extended to combinations of other ILC frameworks simply by: 1) replacing $e_j \mapsto e_j + \hat{J}f^{\mathrm{F}}_j$ for the parametrized ILC update; and 2) adding $f^{\mathrm{B}}_j - f^{\mathrm{B}}_{j+1}$ to the signal-based ILC update. See study (32) for another example in which norm optimal ILC is employed as signal-based ILC, combined with B-ILC.

4. Specifications on Convergence, Tracking-performance and Task-flexibility

In this section, the properties of C-ILC are addressed by specifying the monotonic convergence condition, tracking-performance and task-flexibility. This section constitutes contribution C1.

4.1 Monotonic Convergence From (1), (27) and $f_j = f^{\mathrm{F}}_j + f^{\mathrm{B}}_j$, the propagation of FF parameter is expressed as

$$\theta_{j+1} = (Q^{\mathrm{B}}_{n\times n} - L^{\mathrm{B}}_{n\times N}J_{N\times N}\Psi^{(r)}_{N\times n})\theta_j + L^{\mathrm{B}}_{n\times N}(S_{N\times N}\underline{r} + (\hat{J}_{N\times N} - J_{N\times N})\underline{f}^{\mathrm{F}}_j). \cdots\cdots \quad (29)$$

As $(\hat{J}_{N\times N} - J_{N\times N})\underline{f}^{\mathrm{F}}_j$ is typically negligible, due to $J(e^{i\omega}) - \hat{J}(e^{i\omega}) \approx 0$ for low frequency range ω and $f^{\mathrm{F}}_j(e^{i\omega}) \approx 0$ for high frequency range ω, the monotonic convergence condition for $\|\theta\|_2$ in C-ILC is approximated as that of B-ILC in (13).

Remark 11 Convergence speed of $\|\theta\|_2$ is typically fast for SISO LTI systems[11][33], only requiring about 2 – 5 iterations until convergence.

Additionally, using (1) and the time-domain representation of (28)

$$\underline{f}^{\mathrm{F}}_{j+1} = Q^{\mathrm{F}}_{N\times N}(\underline{f}^{\mathrm{F}}_j + L^{\mathrm{F}}_{N\times N}\underline{e}_j) + \underline{f}^{\mathrm{B}}_j - \underline{f}^{\mathrm{B}}_{j+1}, \cdots\cdots\cdots \quad (30)$$

the propagation of error is expressed as

$$\underline{e}_{j+1} = Q^{\mathrm{F}}_{N\times N}(I_{N\times N} - J_{N\times N}L^{\mathrm{F}}_{N\times N})\underline{e}_j + (I_{N\times N} - Q^{\mathrm{F}}_{N\times N})(S_{N\times N}\underline{r} - J_{N\times N}\underline{f}^{\mathrm{B}}_j). \cdots\cdots \quad (31)$$

As $\|f^{\mathrm{B}}\|_2$ converges monotonically by (29), making the second term of (31) bounded, the monotonic convergence condition of $\|e\|_2$ in C-ILC is approximated as

$$\bar{\sigma}(Q^{\mathrm{F}}_{N\times N}(I_{N\times N} - J_{N\times N}L^{\mathrm{F}}_{N\times N})) < 1, \cdots\cdots\cdots\cdots\cdots \quad (32)$$

which is equivalent to the monotonic convergence condition of F-ILC in (4) when L^{F} is stable and causal[14].

Therefore, the monotonic convergence condition of C-ILC can be approximately tested by (4) and (13), which is desirable compared to the condition of naively combining F-ILC with B-ILC in (19).

4.2 Exceeding Tracking-performance of F-ILC From (31), the asymptotic error $\lim_{j\to\infty} e_j = e_\infty$ of C-ILC can be obtained by a similar discussion in Section 2.3. Under assumption of convergence, $\lim_{j\to\infty} e_j = e_\infty$ is derived as

$$e_\infty = \frac{(1 - Q^{\mathrm{F}})S(1 - GF(\theta_\infty))}{1 - Q^{\mathrm{F}}(1 - L^{\mathrm{F}}J)}r. \cdots\cdots\cdots\cdots\cdots\cdots \quad (33)$$

Comparing (5) and (33), the asymptotic error of C-ILC is multiplied by $(1 - GF(\theta_\infty))$ than that of F-ILC. Therefore, for frequency ω where $Q^{\mathrm{F}}(e^{i\omega}) \neq 1$ and

$$|1 - G(e^{i\omega})F(\theta_\infty, e^{i\omega})| < 1, \cdots\cdots\cdots\cdots\cdots\cdots\cdots \quad (34)$$

C-ILC exceeds the tracking-performance of F-ILC.

While F-ILC can only learn the system dynamics below the bandwidth of robustness filter Q^{F}, B-ILC learn the parameters which fit best to the structure of basis functions. Typically, this leads to B-ILC achieving $F(\theta_\infty) \approx G^{-1}$, not limited to the bandwidth of Q^{F}.

Therefore, it is indicated that for scenarios where the bandwidth of Q^{F} is limited, e.g., when significant modeling error exists, C-ILC exceeds the tracking-performance of F-ILC against repetitive tasks.

4.3 Achieving Task-flexibility of B-ILC In this subsection, the task-flexibility of C-ILC is analyzed by formulating the deviation of parametrized FF learning result θ_∞ from that of B-ILC (14). Assuming convergence of C-ILC confirmed by the previous subsection, (27) and (30) are used to derive the following theorem of θ_∞.

Theorem 1 (Asymptotic FF parameter of C-ILC) *Assuming convergence, the asymptotic FF parameter of C-ILC is*

$$\theta_\infty = (I_{n\times n} - Q^{\mathrm{B}}_{n\times n} + L^{\mathrm{B}}_{n\times N}(I_{N\times N} - \Delta_{N\times N})J_{N\times N}\Psi^{(r)}_{N\times n})^{-1} \times L^{\mathrm{B}}_{n\times N}(I_{N\times N} - \Delta_{N\times N})S\underline{r}, \cdots\cdots (35)$$

where

$$\Delta_{N\times N} = (J_{N\times N} - \hat{J}_{N\times N})(I_{N\times N} - Q^{\mathrm{F}}_{N\times N}(I_{N\times N} - L^{\mathrm{F}}_{N\times N}J_{N\times N}))^{-1} \times Q^{\mathrm{F}}_{N\times N}L^{\mathrm{F}}_{N\times N}. \cdots\cdots (36)$$

Proof. Follows by substituting θ_∞ to θ_j, θ_{j+1} and f^{F}_∞ to f^{F}_j, f^{F}_{j+1} in (27), (30). See Appendix 3 for further details. □

Comparing (14) and (35), the FF parameter deviation between B-ILC and C-ILC is negligible when $\Delta_{N\times N} \approx 0$. For analysis of $\Delta_{N\times N}$, the following corollary is used.

Corollary 1 (Frequency-domain interpretation of $\Delta_{N\times N}$)
When $L^{\mathrm{F}} = \hat{J}^{-1}$, the frequency-domain representation of $\Delta_{N\times N}$ is

$$\Delta(z) = \frac{-Q^{\mathrm{F}}(1 - L^{\mathrm{F}}J)}{1 - Q^{\mathrm{F}}(1 - L^{\mathrm{F}}J)}. \cdots\cdots (37)$$

From (37), when $|Q^{\mathrm{F}}(e^{i\omega})(1 - L^{\mathrm{F}}(e^{i\omega})J(e^{i\omega}))| \ll 1$ is satisfied, $\Delta(e^{i\omega}) \approx 0$ for the entire frequency range ω is achieved. Due to the motivation of designing C-ILC to converge monotonically (32), tested by (4), it is indicated that the deviation of θ_∞ between B-ILC and C-ILC is negligible, i.e., C-ILC achieves identical task-flexibility as B-ILC.

Remark 12 When update for standard B-ILC (11) is used instead of the developed (27), $\Delta(z) = Q^{\mathrm{F}}L^{\mathrm{F}}J(1 - Q^{\mathrm{F}}(1 - L^{\mathrm{F}}J))^{-1} \approx Q^{\mathrm{F}}L^{\mathrm{F}}J$. As $Q^{\mathrm{F}}(e^{i\omega})L^{\mathrm{F}}(e^{i\omega})J(e^{i\omega}) \approx 1$ for frequency range ω below the bandwidth of Q^{F}, which is the main frequency component consisting the FF input, θ_∞ would deviate severely from that of B-ILC. This effect is demonstrated in Appendix 1.

5. Experimental Validation

In this section, the joint parametrized/signal-based ILC framework is experimentally validated with a two-mass motion system. From the previous section, it is especially indicated that C-ILC has further potential to exceed the tracking-performance of F-ILC when the bandwidth of Q^{F} is low. To verify the indication: 1) C-ILC with a sufficiently high bandwidth of Q^{F}; and 2) C-ILC with a low bandwidth of Q^{F}; are validated. For analyzing the results of C-ILC for each scenario, the results are compared with standard parametrized and signal-based ILC frameworks, i.e., F-ILC, B-ILC, using unified conditions stated in Section 5.1. This section constitutes contribution C2.

5.1 Experimental Setup

In this study, the two-mass motion system shown in Fig. 4 is used as a benchmark system for a high-precision positioning stage. The system is controlled at a sampling time of $T_s = 0.25$ ms with a stabilizing FB controller

$$K = \frac{0.3317(1 - 0.9983z^{-1})(1 - 0.8958z^{-1})}{(1 - 0.9851z^{-1})(1 - 0.9540z^{-1})}.$$

The experiments are conducted assuming two modeling scenarios in Fig. 9: 1) one in which the system model is sufficiently constructed including the flexible-mode, enabling the design of a sufficiently high bandwidth Q^{F} ; and 2) another in which the system model only assumes the rigid-body mode, only allowing a low bandwidth Q^{F}. The second scenario can be generalized as an investigation on the effect of under-modeling, which is inevitable for most mechatronic

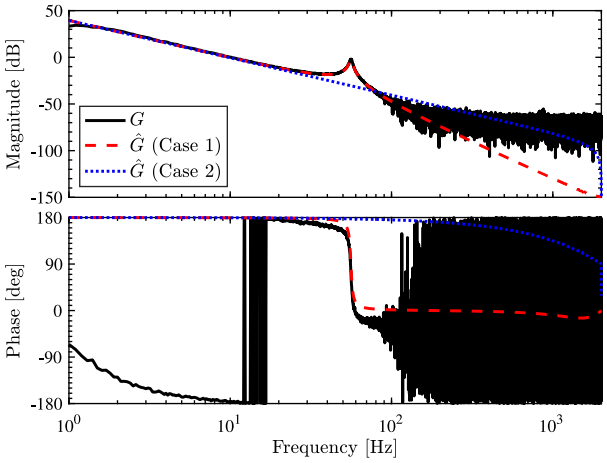

Fig. 9. Identified frequency response data of system G (—) and system model $\hat{G}$ for Case 1 (- -) and Case 2 (····) experiment

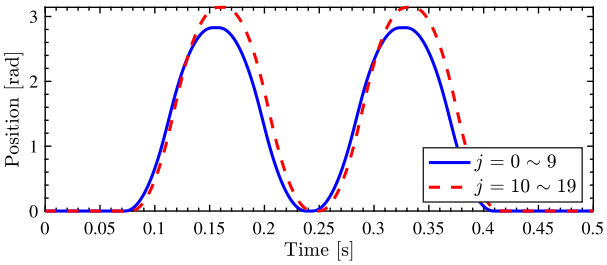

Fig. 10. Reference trajectory used for the experiment. For the first 10 iterations the (—) is used and for the last 10 iterations (- -) is used

systems. The transfer function of each model is as follows.

$$\hat{G}_{(\mathrm{Case1})} = \frac{2.1014\times 10^{-7}z^{-1}(1 + 5.462z^{-1})}{(1 - z^{-1})^2} \times \frac{(1 + 0.4797z^{-1})(1 - 0.1107)}{(1 - 1.989z^{-1} + 0.9965z^{-2})},$$

$$\hat{G}_{(\mathrm{Case2})} = \frac{1.1574\times 10^{-4}z^{-1}(1 + z^{-1})}{(1 - z^{-1})^2}.$$

To evaluate the performance against repetitive tasks ($r_{j+1} = r_j$) and nonrepetitive tasks ($r_{j+1} \neq r_j$), references r_j as shown in Fig. 10 are given for 20 iterations.

In the following experimental results, the results of F-ILC, B-ILC, and developed C-ILC are compared. For fair comparison, following conditions are unified through the validation.

- Q^{F} and L^{F} filters used for F-ILC and C-ILC are designed as, $L^{\mathrm{F}} = \hat{G}^{-1}(1 + \hat{G}K)$ and Q^{F} being: 1) an eighth-order zero phase low-pass filter with a bandwidth of 80 Hz for Case 1; and 2) a fourth-order zero phase low-pass filter with a bandwidth of 18 Hz for Case 2; satisfying the monotonic convergence condition of $\|e\|_2$ in (4).
- Weighting matrices used for the criterion of B-ILC and C-ILC are set as $W_e = I_{N\times N}, W_f = W_{\Delta f} = 0$, satisfying the monotonic convergence condition of $\|\theta\|_2$ in (13).
- The basis functions and FF parameters for B-ILC and C-ILC are selected as: 1) $\Psi^{(r)}_{N\times n} = [\underline{r}, \underline{\dot{r}}, \underline{\ddot{r}}]$ with $\theta =$

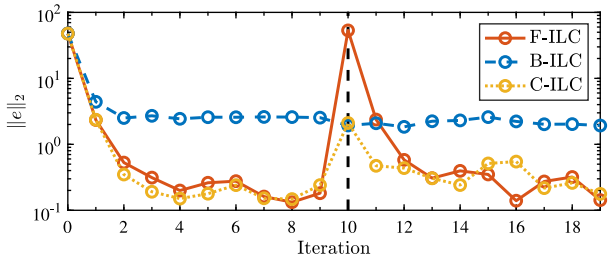

(a) Error norm per iteration.

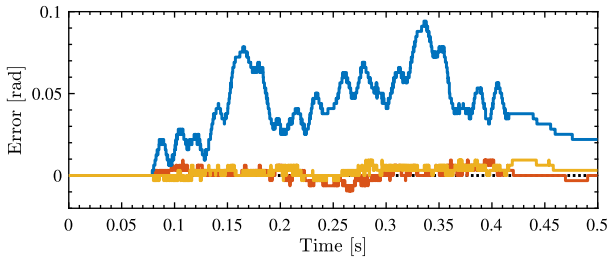

(b) Error signal of final iteration.

Fig. 11. Experimental results with sufficient-order model (Case 1). C-ILC (-o-) chieves high tracking-performance as F-ILC (-o-) for repetitive tasks ($j = 0-9, 11-19$) while achieving identical task-flexibility as B-ILC (-o-) for nonrepetitive tasks ($j = 10$). Both F-ILC (—) and C-ILC (—) reach encoder-resolution error at the final iteration ($j = 19$), while B-ILC (—) exhibits a larger error

$\left[\theta^{\mathrm{vel}}, \theta^{\mathrm{acc}}, \theta^{\mathrm{snap}}\right]^{\top}$ for Case 1; and 2) $\Psi^{(r)}_{N\times n} = \underline{\ddot{r}}$ with $\theta = \theta^{\mathrm{acc}}$ for Case 2; initialized as $\theta_0 = 0$.

- For F-ILC and C-ILC, f_j^{F} is reset to 0 when the task changes at $j = 10$.

5.2 Case 1: Performance with Sufficient-order Model

The experimental results for this case study are shown in Figs. 11–13 and Table 1. 1) The error 2-norm $\|e\|_2$ results shown in Fig. 11 and organized in Table 1; 2) the parametrized learning result of θ_j for 20 iterations shown in Fig. 12; and 3) the learning result of parametrized and signal-based FF input for C-ILC shown in Fig. 13; are summarized with following observations.

- Figure 11(a) shows all ILC frameworks converged at iteration 9 and 19, with slight variation due to trial-varying noise, for example from random encoder pulse variation seen in Fig. 11(b).
- From Table 1, C-ILC exhibits high task-flexibility improving the $\|e_{10}\|_2$ of F-ILC by 96%, with high tracking-performance improving the $\|e_{19}\|_2$ of B-ILC by 91%.
- C-ILC achieves high task-flexibility by performing identical parametrized FF learning as B-ILC displayed in Fig. 12. This is as indicated in Section 4.3.
- C-ILC achieves high tracking-performance by the signal-based FF input successfully learning the residual dynamics uncaptured by the basis functions. This is apparent from Fig. 13, for this scenario f_{19}^{F} likely compensating the nonlinear effect of mass imbalance, amplified by the resonance of the system.

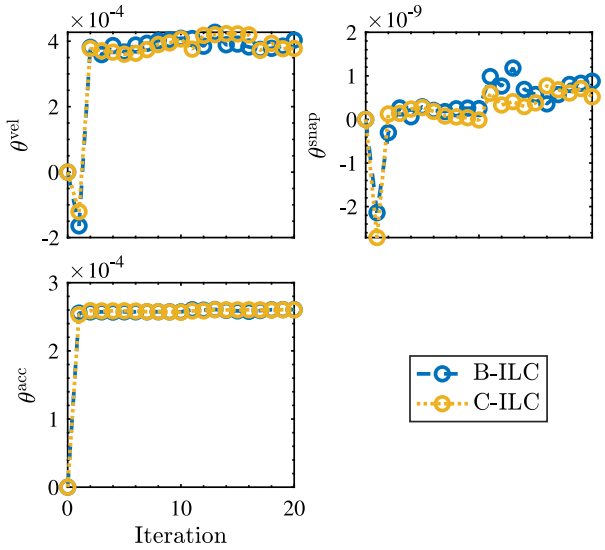

Fig. 12. Comparison of B-ILC (-o-) and C-ILC (-o-) parameter learning results with sufficient-order model (Case 1). Both results of B-ILC and C-ILC achieve identical learning patterns

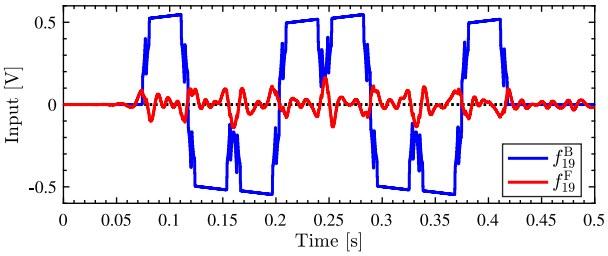

Fig. 13. Comparison of learned FF input for the C-ILC framework with sufficient-order model (Case 1). The input is mainly composed of the parametrized FF input f_{19}^{B} (—), while the signal-based FF input f_{19}^{F} (—) compensates the residual dynamics uncaptured by the basis functions

Table 1. Error norms with sufficient-order model (Case 1)

Method	$\|e_{10}\|_2$	$\|e_{19}\|_2$
F-ILC	53.3036	0.1426
B-ILC	1.9292	1.9268
C-ILC	2.1062	0.1772

- For this scenario, both F-ILC and C-ILC in Fig. 11(b) achieve encoder resolution tracking performance due to a sufficiently high bandwidth $Q^{\mathrm{F}} \approx 1$. (i.e., there is no room for improvement in performance with C-ILC compared to F-ILC.)

To summarize this case study, when the system model is sufficiently accurate such that the bandwidth of Q^{F} is high, C-ILC achieves: 1) high tracking-performance identical to that of F-ILC; with 2) high task-flexibility identical to that of B-ILC.

5.3 Case 2: Performance with Insufficient-order Model

The experimental results for this case study are shown in Figs. 14–16 and Table 2. 1) The error 2-norm $\|e\|_2$ results shown in Fig. 14 and organized in Table 2; 2) the parametrized learning result of θ_j for 20 iterations

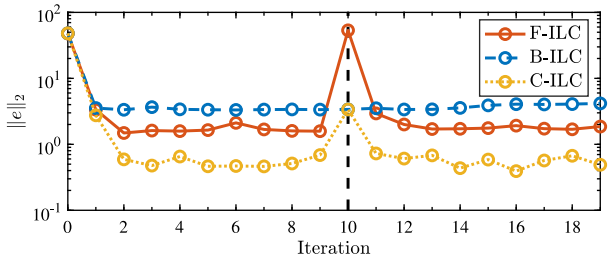

(a) Error norm per iteration.

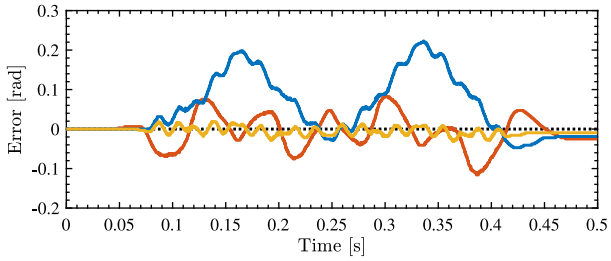

(b) Error signal of final iteration.

Fig. 14. Experimental results with insufficient-order model (Case 2). C-ILC (-o-) achieves high performance exceeding F-ILC (-o-) for repetitive tasks ($j = 0-9, 11-19$) while achieving identical task-flexibility as B-ILC (-o-) for nonrepetitive tasks ($j = 10$). For this scenario, C-ILC (—) achieves tracking-performance exceeding both B-ILC (—) and F-ILC (—) at the final iteration ($j = 19$)

shown in Fig. 15; and 3) the learning result of parametrized and signal-based FF input for C-ILC shown in Fig. 16; are summarized with following observations.

- Figure 14(a) shows all ILC frameworks converged at iteration 9 and 19, with less variation compared to Case 1. This is due to all methods exhibiting larger error as seen in Fig. 14(b), relatively reducing the influence of trial-varying noise.
- From Table 1, C-ILC exhibits high task-flexibility improving the $\|e_{10}\|_2$ of F-ILC by 94%, with high tracking-performance even exceeding the $\|e_{19}\|_2$ of F-ILC by 74%.
- Similar to Case 1, C-ILC achieves high task-flexibility by performing identical parametrized FF learning as B-ILC displayed in Fig. 12.
- Similar to Case 1, C-ILC achieves high tracking-performance by the signal-based FF input in Fig. 13 successfully learning the residual dynamics uncaptured by the basis functions. For this scenario, this is likely the effect of viscous friction, which is proportional to the velocity profile $\dot{r}$.
- As the bandwidth of Q^{F} is low, F-ILC in Fig. 14(b) exhibits a nonnegligible error at iteration 19. This creates room for improvement in C-ILC, indicated from (34).

To summarize this case study, when the system model is insufficient such that the bandwidth of Q^{F} is low, C-ILC achieves: 1) high tracking-performance exceeding that of F-ILC; with 2) high task-flexibility identical to that of B-ILC.

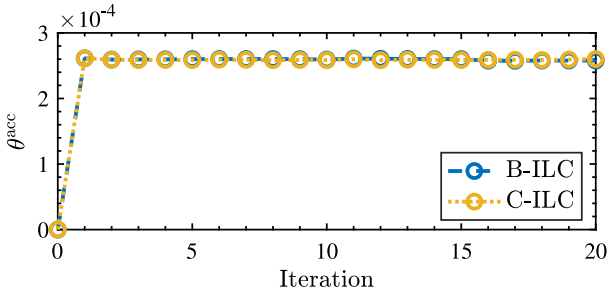

Fig. 15. Comparison of B-ILC (-o-) and C-ILC (-o-) parameter learning results with insufficient-order model (Case 2). Similar to Case 1, both results of B-ILC and C-ILC achieve identical learning patterns

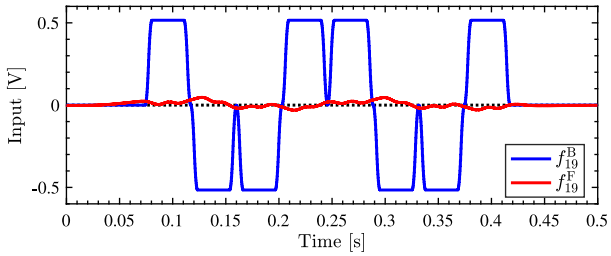

Fig. 16. Comparison of learned FF input for the C-ILC framework with insufficient-order model (Case 2). Similar to Case 1, the input is mainly composed of the parametrized FF input f_{19}^{B} (—), while the signal-based FF input f_{19}^{F} (—) compensates the residual dynamics uncaptured by the basis functions

Table 2. Error norms with insufficient-order model (Case 2)

Method	$\|e_{10}\|_2$	$\|e_{19}\|_2$
F-ILC	53.4406	1.8589
B-ILC	3.3821	4.1671
C-ILC	3.3734	0.4897

6. Conclusion

The joint parametrized/signal-based ILC framework exhibits high task flexibility for nonrepetitive tasks and outstanding tracking performance for repetitive tasks. This is achieved by complementarily combining parametrized with signal-based ILC, avoiding typical interference caused when distinct ILC frameworks are updated in parallel. Theoretical analysis coupled with experimental validation on a two-mass motion system confirms the convergence, task-flexibility and tracking-performance of joint parametrized/signal-based ILC. Especially in terms of tracking-performance, it is verified that joint parametrized/signal-based ILC exceeds simple signal-based ILC when the system model is insufficient, i.e., the bandwidth of the robustness filter Q^{F} is low. This suggests that joint parametrized/signal-based ILC is relevant for practical high-precision motion systems with parasitic dynamics.

For further research, extending the theory to more complicated systems, such as multivariable systems will be investigated.

Acknowledgment

This work is supported in part by JSPS Bilateral Program Number JPJSBP220234403, in part by JSPS Grant-in-Aid

for Scientific Research (B) Program Number 23H01431, and in part by JSPS Grant-in-Aid for JSPS Fellows under Grant 24KJ0959.

References

(1) S. Mishra, J. Coaplen, and M. Tomizuka: "Precision Positioning of Wafer Scanners Segmented Iterative Learning Control for Nonrepetitive Disturbances", *IEEE Control Systems*, Vol.27, No.4, pp.20–25 (2007)

(2) T. Hayashi, H. Fujimoto, Y. Isaoka, and Y. Terada: "Projection-based iterative learning control for ball-screw-driven stage with consideration of rolling friction compensation", *IEEJ Journal of Industry Applications*, Vol.9, No.2, pp.132–139 (2020)

(3) J. Wallén, M. Norrlöf, and S. Gunnarsson: "A framework for analysis of observer-based ILC", *Asian Journal of Control*, Vol.13, No.1, pp.3–14 (2011)

(4) J. Van Zundert and T. Oomen: "On inversion-based approaches for feedforward and ILC", *Mechatronics*, Vol.50, pp.282–291 (2018)

(5) M. Steinbuch, T. Oomen, and H. Vermeulen: "Motion Control, Mechatronics Design, and Moore's Law", *IEEJ Journal of Industry Applications*, Vol.11, No.2, pp.245–255 (2022)

(6) S. Arimoto, S. Kawamura, and F. Miyazaki: "Bettering operation of dynamic systems by learning: A new control theory for servomechanism or mechatronics systems", in The 23rd IEEE Conference on Decision and Control, pp.1064–1069 (1984)

(7) A. Bristow, Douglas, M. Tharayil, and A.G. Andrew: "A survey of iterative learning control", *IEEE Control Systems Magazine*, Vol.26, No.3, pp.96–114 (2006)

(8) K.L. Moore: Iterative learning control for deterministic systems, London: Springer (2012)

(9) N. Kawamura, S. Inoue, T. Zanma, K. Kondo, K. Kenta, K.Z. Liu, and M. Shibata, "Feedback Error Learning-Based Position Control in Position-Sensorless Positioning Servo Systems for IPMSMs", *IEEJ Journal of Industry Applications*, Vol.12, No.4, pp.816–825 (2023)

(10) T. Atsumi, T. Saito, S. Yabui, Y. Nakata, S. Noshiro, and S. Nakadai: "Feedback Controller Optimization for Mechatronic Systems with Unexpected Plant Perturbations Using Support Vector Machine", *IEEJ Journal of Industry Applications*, Vol.13, No.3, pp.270–279 (2024)

(11) S.H. Van Der Meulen, R.L. Tousain, and O.H. Bosgra: "Fixed structure feedforward controller design exploiting iterative trials: Application to a wafer stage and a desktop printer", *Journal of Dynamic Systems, Measurement and Control, Transactions of the ASME*, Vol.130, No.5, pp.1–16 (2008)

(12) J. Bolder and T. Oomen: "Rational basis functions in iterative learning control—With experimental verification on a motion system", *IEEE Transactions on Control Systems Technology*, Vol.23, No.2, pp.722–729 (2015)

(13) T. Mita and E. Kato: "Iterative control and its application to motion control of robot arm—A direct approach to servo-problems", in 1985 24th IEEE Conference on Decision and Control, pp.1393–1398 (1985)

(14) M. Norrlöf and S. Gunnarsson: "Time and frequency domain convergence properties in iterative learning control", *International Journal of Control*, Vol.75, No.14, pp.1114–1126 (2002)

(15) T. Oomen: "Learning for Advanced Motion Control", International Workshop on Advanced Motion Control, pp.65–72 (2020)

(16) X. Ge, J.L. Stein, and T. Ersal: "Frequency-Domain Analysis of Robust Monotonic Convergence of Norm-Optimal Iterative Learning Control", *IEEE Transactions on Control Systems Technology*, Vol.26, No.2, pp.637–651 (2018)

(17) T. Sugie and F. Sakai: "Noise tolerant iterative learning control for a class of continuous-time systems", *Automatica*, Vol.43, No.10, pp.1766–1771 (2007)

(18) T. Oomen and C.R. Rojas: "Sparse iterative learning control with application to a wafer stage: Achieving performance, resource efficiency, and task flexibility", *Mechatronics*, Vol.47, pp.134–147 (2017)

(19) T. Kong, H. Jung, and S. Oh: "Data-Driven Iterative optimization of TDOF Controller with Rational Model", in IEEE International Conference on Mechatronics (ICM), Institute of Electrical and Electronics Engineers Inc., pp.1–6 (2023)

(20) S. Mishra, U. Topcu, and M. Tomizuka: "Optimization-based constrained iterative learning control", *IEEE Transactions on Control Systems Technology*, Vol.19, No.6, pp.1613–1621 (2011)

(21) Y. Chen, B. Chu, and C.T. Freeman: "Generalized iterative learning control using successive projection: Algorithm, convergence, and experimental verification", *IEEE Transactions on Control Systems Technology*, Vol.28, No.6, pp.2079–2091 (2020)

(22) T. Oomen, J. van de Wijdeven, and O. Bosgra: "Suppressing intersample behavior in iterative learning control", *Automatica*, Vol.45, No.4, pp.981–988 (2009)

(23) W. Ohnishi, N. Strijbosch, and T. Oomen: "State-Tracking Iterative Learning Control in Frequency Domain Design for Improved Intersample Behavior", *International Journal of Robust and Nonlinear Control*, Vol.33, No.7, pp.4009–4027 (2023)

(24) M. Mae, M. van Haren, K. Classens, W. Ohnishi, T. Oomen, and H. Fujimoto: "Fixed-structure sampled-data feedforward control for multivariable motion systems", *Mechatronics*, Vol.106, p.103288 (2025)

(25) S. Tien, S. Devasia, and Q. Zou: "Iterative Control of Dynamics-Coupling-Caused Errors in Piezoscanners During High-Speed AFM Operation", *IEEE Transactions on Control Systems Technology*, Vol.13, No.6, pp.921–931 (2005)

(26) L. Aarnoudse and T. Oomen: "Model-Free Learning for Massive MIMO Systems: Stochastic Approximation Adjoint Iterative Learning Control", *IEEE Control Systems Letters*, Vol.5, No.6, pp.1946–1951 (2021)

(27) Y. Maeda and M. Iwasaki: "Frequency-Domain Modeling-Free Iterative Learning Control for Point-To-Point Motion", in 2023 IEEE 32nd International Symposium on Industrial Electronics (ISIE), pp.1–7 (2023)

(28) M. Poot, J. Portegies, N. Mooren, M. van Haren, M. van Meer, and T. Oomen: "Gaussian Processes for Advanced Motion Control", *IEEJ Journal of Industry Applications*, Vol.11, No.3, pp.396–407 (2022)

(29) L. Aarnoudse, J. Kon, W. Ohnishi, M. Poot, P. Tacx, N. Strijbosch, and T. Oomen: "Control-relevant neural networks for feedforward control with preview: Applied to an industrial flatbed printer", *IFAC Journal of Systems and Control*, Vol.27, p.100241 (2024)

(30) K. Tsurumoto, W. Ohnishi, T. Koseki, M. van Haren, and T. Oomen: "Integrated Rational Feedforward in Frequency-Domain Iterative Learning Control for Highly Task-Flexible Motion Control", *IEEE/ASME Transactions on Mechatronics*, Vol.29, No.4, pp.3010–3018 (2024)

(31) M. van Haren, K. Tsurumoto, M. Mae, L. Blanken, W. Ohnishi, and T. Oomen: "A frequency-domain approach for enhanced performance and task flexibility in finite-time ILC", *European Journal of Control*, Vol.80, p.101033 (2024)

(32) K. Tsurumoto, W. Ohnishi, T. Koseki, M. van Haren, and T. Oomen: "Combined Time-Domain Optimization Design for Task-Flexible and High Performance ILC", in 2024 European Control Conference (ECC), pp.1190–1195 (2024)

(33) L. Blanken, F. Boeren, D. Bruijnen, and T. Oomen: "Batch-To-Batch Rational Feedforward Control: From Iterative Learning to Identification Approaches, with Application to a Wafer Stage", *IEEE/ASME Transactions on Mechatronics*, Vol.22, No.2, pp.826–837 (2017)

(34) R.M. Schmidt, G. Schitter, A. Rankers, and J. Van Eijk: *The Design of High Performance Mechatronics: High-Tech Functionality by Multidisciplinary System Integration: 3rd revised edition*, IOS Press (2020)

(35) K. Sakata, H. Asaumi, K. Hirachi, K. Saiki, and H. Fujimoto: "Self Resonance Cancellation Techniques for a Two-Mass System and Its Application to a Large-Scale Stage", *IEEJ Journal of Industry Applications*, Vol.3, No.6, pp.455–462 (2014)

(36) T. Oomen: "Advanced Motion Control for Precision Mechatronics: Control, Identification, and Learning of Complex Systems", *IEEJ Journal of Industry Applications*, Vol.7, No.2, pp.127–140 (2018)

(37) A.J. Fleming and K.K. Leang: *Design, modeling and control of nanopositioning systems*, Switzerland: Springer International Publishing (2014)

(38) S. Gunnarsson and M. Norrlöf: "On the design of ILC algorithms using optimization", *Automatica*, Vol.37, pp.2011–2016 (2001)

(39) D.H. Owens: *Iterative Learning Control: An Optimization Paradigm*, Springer (2015)

(40) J. Van De Wijdeven and O.H. Bosgra: "Using basis functions in iterative learning control: analysis and design theory", *International Journal of Control*, Vol.83, No.4, pp.661–675 (2010)

Appendix

1. Excessive Learning by Naively Combining F-ILC and B-ILC Update Laws

Excessive FF learning of simultaneously applying the update law

$$f^{\mathrm{F}}_{j+1} = Q^{\mathrm{F}}(f^{\mathrm{F}}_j + L^{\mathrm{F}} e_j), \quad \cdots\cdots\cdots\cdots\cdots\cdots (\mathrm{A1})$$

$$\theta_{j+1} = Q^{\mathrm{B}}_{n\times n}\theta_j + L^{\mathrm{B}}_{n\times N}\underline{e}_j, \quad \cdots\cdots\cdots\cdots\cdots\cdots (\mathrm{A2})$$

from (2) and (11), and combining it as $f_{j+1} = f^{\mathrm{F}}_{j+1} + F(\theta_{j+1})r$ is demonstrated by a simulation study. For the simulation, true system and system model are assumed as $\hat{G}$ from Case 1 and Case 2 in Section 5, and learning conditions from Case 2

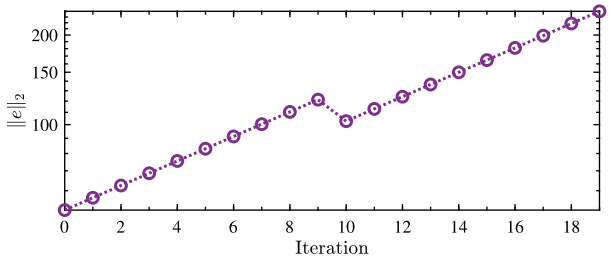

(a) Error norm per iteration.

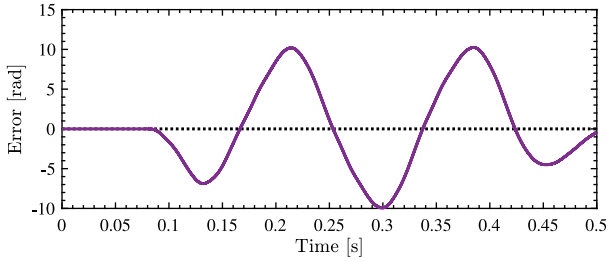

(b) Error signal of final iteration.

app. Fig. 1. Simulation results with naive combination of F-ILC (2) and B-ILC (11) updates. Naive combination (-⊖-) leads to divergent learning, resulting to tracking error (—) at the final iteration ($j = 19$) inferior to feedback without any feedforward ($j = 0$)

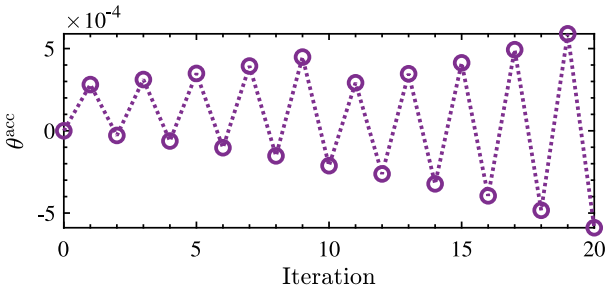

app. Fig. 2. Divergent parameter learning results (-⊖-) with naive combination of F-ILC (2) and B-ILC (11) updates

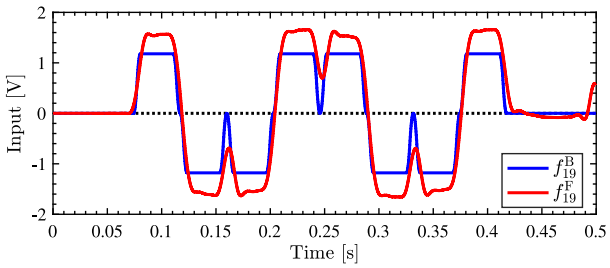

app. Fig. 3. Comparison of learned FF input with naive combination of F-ILC (2) and B-ILC (11). Unlike app. Fig. 16, both f^{B}_{19} (—) and f^{F}_{19} (—) try to learn the system dynamics, resulting to excessive learning

are applied.

The simulation results for are shown in app. Figs. 1, 2 and 3. 1) The error 2-norm $\|e\|_2$ for 20 iterations and signal e_{19} shown in app. Fig. 1; 2) the parametrized learning result of θ_j for 20 iterations shown in app. Fig. 2; and 3) the learning result of parametrized and signal-based FF input shown in app. Fig. 3; are summarized with following observations.

- app. Fig. 1 shows the divergence of naive combination. The result demonstrates that not only does it perform inferior to all methods in app. Fig. 14, but it is outperformed by simple feedback without any feedforward.
- Parametrized FF learning of naive combination in app. Fig. 2 diverges, far ideal from that of B-ILC in app. Fig. 15. This is due to the additional signal-based FF update of f^{F}_{j+1} (A1) severely interacting with the parametrized FF update of θ_{j+1} (A2).
- app. Fig. 3 shows the FF input $f_{19} = f^{\mathrm{B}}_{19} + f^{\mathrm{F}}_{19}$ of the naive combination. Unlike the results in app. Fig. 16, both f^{B} and f^{F} try to learn the system dynamics, leading to excessive learning.

Hence, even when the updates of F-ILC (A1) and B-ILC (A2) are individually designed to satisfy the monotonic convergence condition (4) and (13), naively combining the updates may result in divergent learning as indicated in (19).

2. Proof of Definition 4

From (1), (7) and (25), $\underline{e}^{\theta}_{j+1}$ in (24) can be written as

$$\underline{e}^{\theta}_{j+1} = \underline{e}_j + J_{N\times N}(\underline{f}^{\mathrm{F}}_j + \Psi^{(r)}_{N\times n}(\theta_j - \theta_{j+1})). \cdots\cdots\cdots \text{(A3)}$$

Any solution θ_{j+1} to optimization problem (10) necessarily satisfies $\partial V(\theta_{j+1})/\partial\theta_{j+1} = 0$. Evaluating this condition for criterion (24) with (A3) gives

$$\left(\frac{\partial \underline{\hat{e}}^{\theta}_{j+1}}{\partial\theta_{j+1}}\right)^{\top} W_e \underline{\hat{e}}^{\theta}_{j+1} + \left(\frac{\partial \underline{f}^{\mathrm{B}}_{j+1}}{\partial\theta_{j+1}}\right)^{\top} W_f \underline{f}^{\mathrm{B}}_{j+1}$$
$$+ \left(\frac{\partial(\underline{f}^{\mathrm{B}}_{j+1} - \underline{f}^{\mathrm{B}}_{j})}{\partial\theta_{j+1}}\right)^{\top} W_{\Delta f}(\underline{f}^{\mathrm{B}}_{j+1} - \underline{f}^{\mathrm{B}}_{j}) = 0, \cdots\cdots\cdots \text{(A4)}$$

where the gradient of $\underline{\hat{e}}^{\theta}_{j+1}$, $\underline{f}^{\mathrm{B}}_{j+1}$, and $\underline{f}^{\mathrm{B}}_{j+1} - \underline{f}^{\mathrm{B}}_{j}$ are given by

$$\left(\frac{\partial \underline{\hat{e}}^{\theta}_{j+1}}{\partial\theta_{j+1}}\right) = \hat{J}_{N\times N}\Psi^{(r)}_{N\times n}, \cdots\cdots\cdots\cdots\cdots\cdots\cdots \text{(A5a)}$$
$$\left(\frac{\partial \underline{f}^{\mathrm{B}}_{j+1}}{\partial\theta_{j+1}}\right) = \left(\frac{\partial(\underline{f}^{\mathrm{B}}_{j+1} - \underline{f}^{\mathrm{B}}_{j})}{\partial\theta_{j+1}}\right) = \Psi^{(r)}_{N\times n}. \cdots\cdots\cdots\cdots \text{(A5b)}$$

By substituting (7), (A3) and (A5) into (A4), we obtain

$$\theta_{j+1} = Q^{\mathrm{B}}_{n\times n}\theta_j + L^{\mathrm{B}}_{n\times N}(\underline{e}_j + \hat{J}_{N\times N}\underline{f}^{\mathrm{F}}_j),$$

where

$$L^{\mathrm{B}}_{n\times N} = R^{-1}_{n\times n}\Psi^{(r)\top}_{N\times n}\hat{J}^{\top}_{N\times N}W_e, \cdots\cdots\cdots\cdots\cdots\cdots\cdots \text{(A6a)}$$
$$Q^{\mathrm{B}}_{n\times n} = R^{-1}_{n\times n}\Psi^{(r)\top}_{N\times n}(\hat{J}^{\top}_{N\times N}W_e\hat{J}_{N\times N} + W_{\Delta f})\Psi^{(r)}_{N\times n}, \cdots\cdots\cdots\cdots\cdots\cdots\cdots \text{(A6b)}$$
$$R_{n\times n} = \Psi^{(r)\top}_{N\times n}(\hat{J}^{\top}_{N\times N}W_e\hat{J}_{N\times N} + W_f + W_{\Delta f})\Psi^{(r)}_{N\times n},$$

3. Proof of Theorem 1

Under assumption of C-ILC convergence, (1), and (7), the following relationship holds from (27) and (30).

$$\underline{f}^{\mathrm{F}}_{\infty} = Q^{\mathrm{F}}_{N\times N}(I_{N\times N} - L^{\mathrm{F}}_{N\times N}J_{N\times N})\underline{f}^{\mathrm{F}}_{\infty}$$
$$+ Q^{\mathrm{F}}_{N\times N}L^{\mathrm{F}}_{N\times N}(S_{N\times N}\underline{r} - J_{N\times N}\Psi^{(r)}_{N\times n}\theta_{\infty})$$
$$= (I_{N\times N} - Q^{\mathrm{F}}_{N\times N}(I_{N\times N} - L^{\mathrm{F}}_{N\times N}J_{N\times N}))^{-1}$$

$$\times Q^{\mathrm{F}}_{N\times N} L^{\mathrm{F}}_{N\times N}(S_{N\times N}\underline{r} - J_{N\times N}\Psi^{(r)}_{N\times n}\theta_\infty), \cdots\cdots \text{(A7)}$$

$$\theta_\infty = (Q^{\mathrm{B}}_{n\times n} - L^{\mathrm{B}}_{n\times N} J_{N\times N}\Psi^{(r)}_{N\times n})\theta_\infty + L^{\mathrm{B}}_{n\times N}(S_{N\times N}\underline{r} - (J_{N\times N} - \hat{J}_{N\times N})\underline{f}^{\mathrm{F}}_\infty). \cdots\cdots\cdots \text{(A8)}$$

By substituting (A7), (A8) can be written as

$$\begin{aligned}\theta_\infty &= (Q^{\mathrm{B}}_{n\times n} - L^{\mathrm{B}}_{n\times N} J_{N\times N}\Psi^{(r)}_{N\times n})\theta_\infty \\ &\quad + L^{\mathrm{B}}_{n\times N}(S_{N\times N}\underline{r} - \Delta_{N\times N}(S_{N\times N}\underline{r} - J_{N\times N}\Psi^{(r)}_{N\times n}\theta_\infty)), \\ &= (I_{n\times n} - Q^{\mathrm{B}}_{n\times n} + L^{\mathrm{B}}_{n\times N}(I_{N\times N} - \Delta_{N\times N})J_{N\times N}\Psi^{(r)}_{N\times n})^{-1} \\ &\quad \times L^{\mathrm{B}}_{n\times N}(I_{N\times N} - \Delta_{N\times N})S_{N\times N}\underline{r}\end{aligned}$$

where

$$\begin{aligned}\Delta_{N\times N} &= (J_{N\times N} - \hat{J}_{N\times N}) \\ &\quad \times (I_{N\times N} - Q^{\mathrm{F}}_{N\times N}(I_{N\times N} - L^{\mathrm{F}}_{N\times N} J_{N\times N}))^{-1} Q^{\mathrm{F}}_{N\times N} L^{\mathrm{F}}_{N\times N}.\end{aligned}$$

Kentaro Tsurumoto (Student Member) received the M.Sc. degree in Department of Electrical Engineering and Information Systems from The University of Tokyo, Japan, in 2024. He is currently pursuing a Ph.D. degree in the Department of Electrical Engineering and Information Systems, Graduate School of Engineering, The University of Tokyo. He is a recipient of the IEEJ Industry Applications Society Excellent Presentation Award (SAMCON 2022). He is a student member of IEEE. His research interests include high-precision motion control and learning control.

Wataru Ohnishi (Senior Member) received the B.E., M.S., and Ph.D. degrees from The University of Tokyo, Japan, in 2013, 2015, and 2018, respectively. He is currently an associate professor with the Department of Electrical Engineering and Information Systems, Graduate School of Engineering, The University of Tokyo. He held a visiting position at the Eindhoven University of Technology. He is a member of IEEE. His research interests include high-precision motion control and optimization.

Takafumi Koseki (Fellow) received his Ph.D. degree from The University of Tokyo, Japan, in 1992. He is currently a professor with the Department of Electrical Engineering and Information Systems, Graduate School of Engineering, The University of Tokyo. He is a member of IEEE, Japan Society of Mechanical Engineering, Japan Society of Applied Electromagnetics and Mechanics, Japan Society of Precision Engineering, Japan Railway Electrical Engineering Association. His research interests include public transport systems, particularly linear drives, and the analysis and control of traction systems.

Johan Kon (Non-member) received the M.Sc. degree (2021, cum laude) and Ph.D. degree (2025) in Mechanical Engineering from the Eindhoven University of Technology, Eindhoven, The Netherlands. His research interests include feedforward control and inverse system identification with neural networks applied to high precision mechatronic systems.

Maurice Poot (Non-member) received the M.Sc. degree and Ph.D. degree in Mechanical Engineering from the Eindhoven University of Technology, Eindhoven, The Netherlands in 2019 and 2024, respectively. His research interest includes learning control and Gaussian processes for precision mechatronics.

Tom Oomen (Non-member) received the M.Sc. degree (cum laude) and Ph.D. degree from the Eindhoven University of Technology, Eindhoven, The Netherlands. He is currently a professor with the Department of Mechanical Engineering at the Eindhoven University of Technology. He is also a part-time full professor with the Delft University of Technology. He held visiting positions at KTH, Stockholm, Sweden, and at The University of Newcastle, Australia. He is a recipient of the 7th Grand Nagamori Award, the Corus Young Talent Graduation Award, the IFAC 2019 TC 4.2 Mechatronics Young Research Award, the 2015 IEEE Transactions on Control Systems Technology Outstanding Paper Award, the 2017 IFAC Mechatronics Best Paper Award, the 2019 IEEJ Journal of Industry Applications Best Paper Award, and recipient of a Veni and Vidi personal grant. He is Senior Editor of the IEEE Control Systems Letters (L-CSS) and Co-Editor-in-Chief of IFAC Mechatronics. He has also served as Associate Editor for IFAC Mechatronics, IEEE Transactions on Control Systems Technology, and IEEE Control Systems Letters (L-CSS). He is a member of the Eindhoven Young Academy of Engineering. His research interests are in the field of data-driven modeling, learning, and control, with applications in precision mechatronics.